Parasitology Research (2019) 118:2651–2667
https://doi.org/10.1007/s00436-019-06381-z

PROTOZOOLOGY - ORIGINAL PAPER

Motility and cytoskeletal organisation in the archigregarine *Selenidium pygospionis* (Apicomplexa): observations on native and experimentally affected parasites

Magdaléna Kováčiková[1] · Gita G. Paskerova[2] · Andrei Diakin[1] · Timur G. Simdyanov[3] · Naděžda Vaškovicová[4] · Andrea Valigurová[1]

Received: 5 January 2019 / Accepted: 19 June 2019 / Published online: 3 July 2019

Abstract

Representatives of Apicomplexa perform various kinds of movements that are linked to the different stages of their life cycle. Ancestral apicomplexan lineages, including gregarines, represent organisms suitable for research into the evolution and diversification of motility within the group. The vermiform trophozoites and gamonts of the archigregarine *Selenidium pygospionis* perform a very active type of bending motility. Experimental assays and subsequent light, electron, and confocal microscopic analyses demonstrated the fundamental role of the cytoskeletal proteins actin and tubulin in *S. pygospionis* motility and allowed us to compare the mechanism of its movement to the gliding machinery (the so-called glideosome concept) described in apicomplexan zoites. Actin-modifying drugs caused a reduction in the movement speed (cytochalasin D) or stopped the motility of archigregarines completely (jasplakinolide). Microtubule-disrupting drugs (oryzalin and colchicine) had an even more noticeable effect on archigregarine motility. The fading and disappearance of microtubules were documented in ultrathin sections, along with the formation of α-tubulin clusters visible after the immunofluorescent labelling of drug-treated archigregarines. The obtained data indicate that subpellicular microtubules most likely constitute the main motor structure involved in *S. pygospionis* bending motility, while actin has rather a supportive function.

Keywords Actin · Cytoskeletal drugs · Microtubules · Motility · Ultrastructure · α-Tubulin

Andrei Diakin was deceased on 5 November 2018

Section Editor: David S. Lindsay

Electronic supplementary material The online version of this article (https://doi.org/10.1007/s00436-019-06381-z) contains supplementary material, which is available to authorized users.

✉ Magdaléna Kováčiková
kovacikova@sci.muni.cz

[1] Department of Botany and Zoology, Faculty of Science, Masaryk University, Kotlářská 2, 611 37 Brno, Czech Republic

[2] Department of Invertebrate Zoology, Faculty of Biology, Saint-Petersburg State University, Universitetskaya emb. 7/9, St. Petersburg, Russian Federation 199034

[3] Department of Invertebrate Zoology, Faculty of Biology, Lomonosov Moscow State University, Leninskiye Gory 1-12, Moscow, Russian Federation 119234

[4] Institute of Scientific Instruments, The Czech Academy of Sciences, Královopolská 147, 612 64 Brno, Czech Republic

Introduction

Since apicomplexans are exclusively parasitic unicellular organisms with a global medical and economic impact (e.g. *Toxoplasma gondii*, *Plasmodium* spp.), the mechanisms of their motility and host cell invasion have been studied intensively. The apical complex, characteristic of apicomplexan zoites, is responsible for the host-cell recognition and invasion (Dubremetz et al. 1998). The three-membrane pellicle covering the zoite surface is composed of a plasma membrane underlain by flattened alveoli (the inner membrane complex (IMC)). This cell cortex is associated with numerous cytoskeletal elements such as subpellicular microtubules, a network of intermediate filamentous proteins, actin, and myosin (Morrissette and Sibley 2002a). Apicomplexan zoites perform a substrate-dependent gliding motility achieved via an actomyosin motor system, which is intimately associated with their pellicle (Soldati et al. 2004; Tardieux and Baum 2016).

In basal apicomplexan ancestral groups, however, the exact mechanism of motility remains unclear.

Gregarines are the ancestral lineages of apicomplexans, with their localisation restricted to the intestine, gonads, or body cavities of invertebrate and urochordate hosts (Schrével and Desportes 2015), and exhibit various modes of movements. Archigregarines are found exclusively in marine environments and inferred, on the basis of their plesiomorphic characteristics, to be the most ancestral representative of gregarines and perhaps apicomplexans as a whole (Leander 2008; Schrével 1971a). The life cycle of archigregarines belonging to the family Selenidiidae Brasil, 1907, takes place in the intestine of polychaetes, sipunculids, and some hemichordates (Schrével and Desportes 2015). The trophozoites of *Selenidium* spp., similar in cell morphology to the invasive apicomplexan stages (zoites, sporozoites), use to be called "hypersporozoites" or "hypertrophied zoites" (Schrével 1971a; Schrével and Desportes 2015; Schrével et al. 2016). They are covered by a typical apicomplexan three-layered pellicle and possess an apical complex (Schrével 1971a, b; Simdyanov and Kuvardina 2007). *Selenidium* archigregarines exhibit pendular, rolling, coiling, and so-called nematode-like movement (Fowell 1936; Leander 2007; Leander et al. 2003; Paskerova et al. 2018; Schrével 1971a; Schrével and Philippe 1993; Schrével et al. 2016; Simdyanov and Kuvardina 2007). These movements are supposed to be facilitated by regular sets of subpellicular microtubules (Schrével et al. 1974; Stebbings et al. 1974).

The engagement of cytoskeletal proteins (actin, myosin, and tubulin) in motility was previously investigated predominantly in eugregarines from insect hosts that exhibited linear gliding (Ghazali and Schrével 1993; Ghazali et al. 1989; Heintzelman 2004; Heintzelman and Mateer 2008; Kováčiková et al. 2018; Valigurová et al. 2013); only a few studies deal with motility in archigregarines. The role of subpellicular microtubules in *Selenidium* motility was studied using experimental assays with colchicine and urea influencing tubulin polymerisation (Schrével et al. 1974; Stebbings et al. 1974). Other studies used immunofluorescence microscopy to localise α-tubulin and α-actinin in the cell cortex of *Selenidium* representatives. Both these proteins were discussed regarding the motility of archigregarines (Ghazali and Schrével 1995; Wakeman et al. 2014).

The present study focuses on the movement of *Selenidium pygospionis* Paskerova et al. 2018, a parasite of *Pygospio elegans* Claparède, 1863 (Polychaeta, Spionidae). A combination of light, electron, and confocal microscopic approaches, enriched by experimental motility assays on trophozoites and gamonts isolated from host intestine, enabled us to verify the fundamental role of actin and tubulin in archigregarine motility, the mechanism of which presumably differs from the gliding mechanism described for apicomplexan zoites.

Material and methods

The host organisms, polychaetes *Pygospio elegans* (Spionidae), were collected at the littoral zone near the White Sea Biological Station of Lomonosov Moscow State University (Velikaja Salma, Kandalaksha Bay, White Sea, 66° 33.200′ N, 33° 6.283′ E) during the years 2014–2016. Prior to dissection, the animals were stored in small containers at + 10 °C with periodically changed seawater. The dissection of polychaetes and isolation of the archigregarine *Selenidium pygospionis* were performed in Millipore-filtered (0.22 μm) seawater with the help of entomological needles and hand-drawn glass pipettes under an MBS-1 stereomicroscope (LOMO, Russia). Parasites isolated from the host intestine were transferred to embryo dishes for careful washing in Millipore-filtered seawater and subsequent procedures.

Light microscopy and experimental assays

For experimental assays, archigregarines were divided among several embryo dishes with a 30-mm diameter cavity. Jasplakinolide (a cytotoxic natural reagent inducing actin polymerisation and stabilising existing filaments—JAS; Cat. No. J7473, Invitrogen, Czech Republic) and cytochalasin D (a cell-permeable alkaloid inhibiting actin polymerisation and disrupting existing actin microfilaments; Cat. No. PHZ1063, Invitrogen, Czech Republic) were applied at a concentration of 30 μM to investigate the actin involvement in archigregarines motility. Microtubule-disrupting/antimitotic agents, 10 and 30 μM oryzalin (Cat. No. 36182, Sigma-Aldrich, Czech Republic) and 100 mM colchicine (Cat. No. C3915, Sigma-Aldrich, Czech Republic), were used to affect the subpellicular microtubules. Colchicine was reconstituted directly in filtered seawater, while oryzalin, jasplakinolide, and cytochalasin D were reconstituted in dimethyl sulfoxide (DMSO; Cat. No. 276855, Sigma-Aldrich, Czech Republic) to prepare a 1 mM stock solution and afterwards diluted in filtered seawater to prepare a final concentration (10 or 30 μM) of working solution. The initial concentrations of all drugs were set on the basis of experimental data published in Valigurová et al. (2013, 2017). Controls were performed in filtered seawater and corresponding concentrations of DMSO in filtered seawater. Three repetitions of each experimental assay were performed over a period of 3 years. For each drug tested, 100–150 individuals of *S. pygospionis* were used in controls and in each individual motility assay. For light microscopic observations and the documentation of *S. pygospionis* motility at set time intervals, small samples of control and drug-treated parasites were transferred from experimental assays in embryo dishes to microscopic slides. Their motility was monitored using a Leica DM 2000 light microscope connected to a DFC 420 digital camera (Leica Microsystems, Germany). At the end of the experiments,

parasites from each assay were equally divided into three portions and fixed for microscopic analyses (scanning and transmission electron microscopy and confocal laser scanning microscopy).

Transmission electron microscopy

A suspension of parasites was fixed in an ice bath in 2.5% (*v*/*v*) glutaraldehyde in cacodylate buffer (0.05 M; pH = 7.4). The osmolality of the fixative was set to 750 mOsm by the addition of 1.28% NaCl (according to the salinity of the host habitat). Specimens were then rinsed 3× for 15 min and post-fixed in 1% (*w*/*v*) OsO_4 for 2 h in the same buffer as used for fixation with adapted osmolality to 750 mOsm. A portion of the samples was fixed in an ice bath in 2.5% (*v*/*v*) glutaraldehyde in filtered seawater and rinsed 3× for 15 min in cacodylate buffer (0.2 M; pH = 7.4) then post-fixed in 1% (*w*/*v*) OsO_4 for 2 h. Alternatively, parasites were fixed with 3% glutaraldehyde-ruthenium red [0.15% (*w*/*v*) stock water solution] in cacodylate buffer (0.1 M; pH = 7.4) and post-fixed in 1% (*w*/*v*) OsO_4-ruthenium red in the same buffer for 2 h. After rinsing 3× for 15 min in the washing buffers (according to the fixative used), suspensions of archigregarines were embedded in agar [2% (*w*/*v*) in distilled water; 62 °C]. Afterwards, the samples were dehydrated in an ethanol series and embedded in Epon (Polybed 812). The ultrathin sections were obtained with diamond knives using a Leica EM UC6 ultramicrotome (Leica Microsystems, Germany) and stained with uranyl acetate and lead citrate. The sections were examined under a TEM-1010 (JEOL, Japan).

Scanning electron microscopy

Specimens were fixed in 5% (*v*/*v*) glutaraldehyde in cacodylate buffer (0.2 M; pH = 7.4), washed 3× for 15 min in cacodylate buffer, post-fixed in 1% (*w*/*v*) OsO_4 for 2 h in the same buffer, and finally washed 3× for 15 min in cacodylate buffer. After dehydration in an ethanol series, parasites were critical point-dried with CO_2, coated with gold, and observed using a JSM-7401F (JEOL, Japan).

Confocal laser scanning microscopy (CLSM)

Suspensions of archigregarines were fixed for 45 min in freshly prepared 4% paraformaldehyde (PFA) in 0.1 M phosphate-buffered saline (PBS) at room temperature and then washed 3× for 15 min in 0.1 M PBS before further processing. Individuals incubated in JAS were rinsed before fixation to prevent the competitive inhibition of phalloidin binding. Specimens were afterwards permeabilised with 0.5% Triton X-100 (Sigma-Aldrich, Czech Republic) for 15 min. The direct fluorescence of filamentous actin (F-actin) was performed using phalloidin-tetramethylrhodamine B isothiocyanate (phalloidin-TRITC; Cat. No. P1951, Sigma-Aldrich, Czech Republic) wherein the samples were incubated overnight at room temperature and then washed 3× for 10 min in 0.1 M PBS. For indirect immunofluorescence, the specimens were incubated overnight at 4 °C either with mouse monoclonal IgG anti-actin raised against *Dictyostelium* actin or recognising actin in *Toxoplasma gondii* and *Plasmodium* sp. (provided by Prof. Dominique Soldati-Favre, University of Geneva) or with mouse monoclonal anti-α-tubulin (dilution 1:1000; Cat. No. T5168, Sigma-Aldrich, Czech Republic), both in PBS with 0.1% BSA. After washing 3× for 10 min in 0.1 M PBS, the specimens were incubated at 37 °C for 4 h with FITC-conjugated anti-mouse (dilution 1:125; Cat. No. F1010, Sigma-Aldrich, Czech Republic) in PBS with 1% BSA and then washed again. For the localisation of the cell nucleus, the specimens were stained with Hoechst 33342 (Cat. No. H1399, Molecular Probes, Czech Republic) for 1 h and then washed 3× for 10 min in 0.1 M PBS. The samples were mounted in VECTASHIELD Hard Set Mounting Medium (Cat. No. H-1400; Vector Laboratories, USA). Controls were incubated with a secondary antibody alone, i.e. without primary antibody. Preparations were examined under an Olympus IX81 FVBF-2 microscope equipped with a laser-scanning Fluo View 500 confocal unit (Fluo View 3.4 software; Olympus, Japan) and DP70 digital camera. Fluorescence was visualised using TRITC (phalloidin/544 nm) and FITC (anti-actin, anti-α-tubulin/457–515 nm) lasers sets. Micrographs of all specimens (particular staining and controls) were obtained under identical image capture conditions (filters, laser intensity). Some micrographs were processed using Fiji software (an image processing package based on ImageJ developed at the National Institutes of Health).

Results

Motility and cytoskeletal organisation in native *Selenidium pygospionis*

S. pygospionis detached from the host tissue exhibited a regular bending or nematode-like non-progressive movement. The bending wave started at the archigregarine hook-shaped apical end and proceeded posteriorly along the entire cell. Depending on the trophozoite/gamont size, one to three bends propagating along the cell were observed (Fig. 1a–e) (Online Resource 1). The beating frequency of detached parasites was, on average, 0.35 ± 0.04 beats/s (the average time between two beats was 2.87 ± 0.33 s; $n = 8$).

The pellicle of the slightly flattened, vermiform *S. pygospionis* formed broad longitudinal folds, separated by grooves (Fig. 1f–h) with numerous irregularly distributed micropores (Figs. 1g, j, 2a, b). Additional small transversal folds

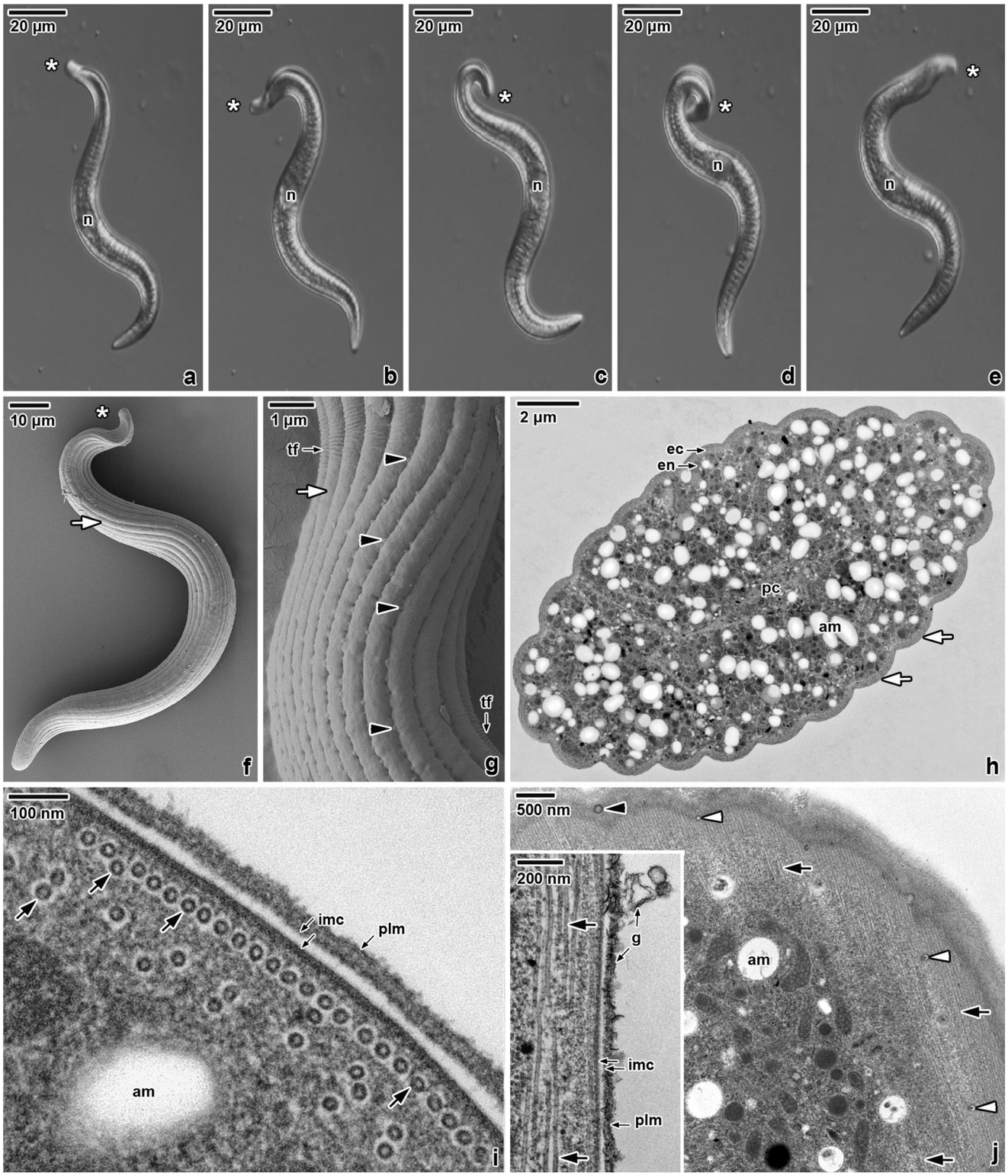

Fig. 1 Motility, surface morphology, and cortex organisation in *Selenidium pygospionis*. **a**–**e** A series of micrographs showing sequences of bending motility of *S. pygospionis* (3 bends along the cell); LM. **f** Detached archigregarine with a pellicle organised into broad longitudinal folds; SEM. **g** Surface morphology at higher magnification; SEM. **h** General view of cross-sectioned archigregarine demonstrating organisation of longitudinal folds; TEM. **i** Detail of cell cortex with layers of subpellicular microtubules in cross-sections; TEM. **j** Superficial tangential section of cortex showing the organisation of microtubules, micropores, vesicular ducts, and a glycocalyx coat. Inset shows longitudinally sectioned microtubules in detail; TEM, Inset—RR TEM. am, amylopectin; asterisk, apical end; black arrow, microtubules; black arrowhead, micropore; ec, ectoplasm; en, endoplasm; g, glycocalyx; imc, inner membrane complex; n, nucleus; pc, electron-light area of the cytoplasm; plm, plasma membrane; tf, transversal folds; white arrow, folds; white arrowhead, duct connected to vesicular structure

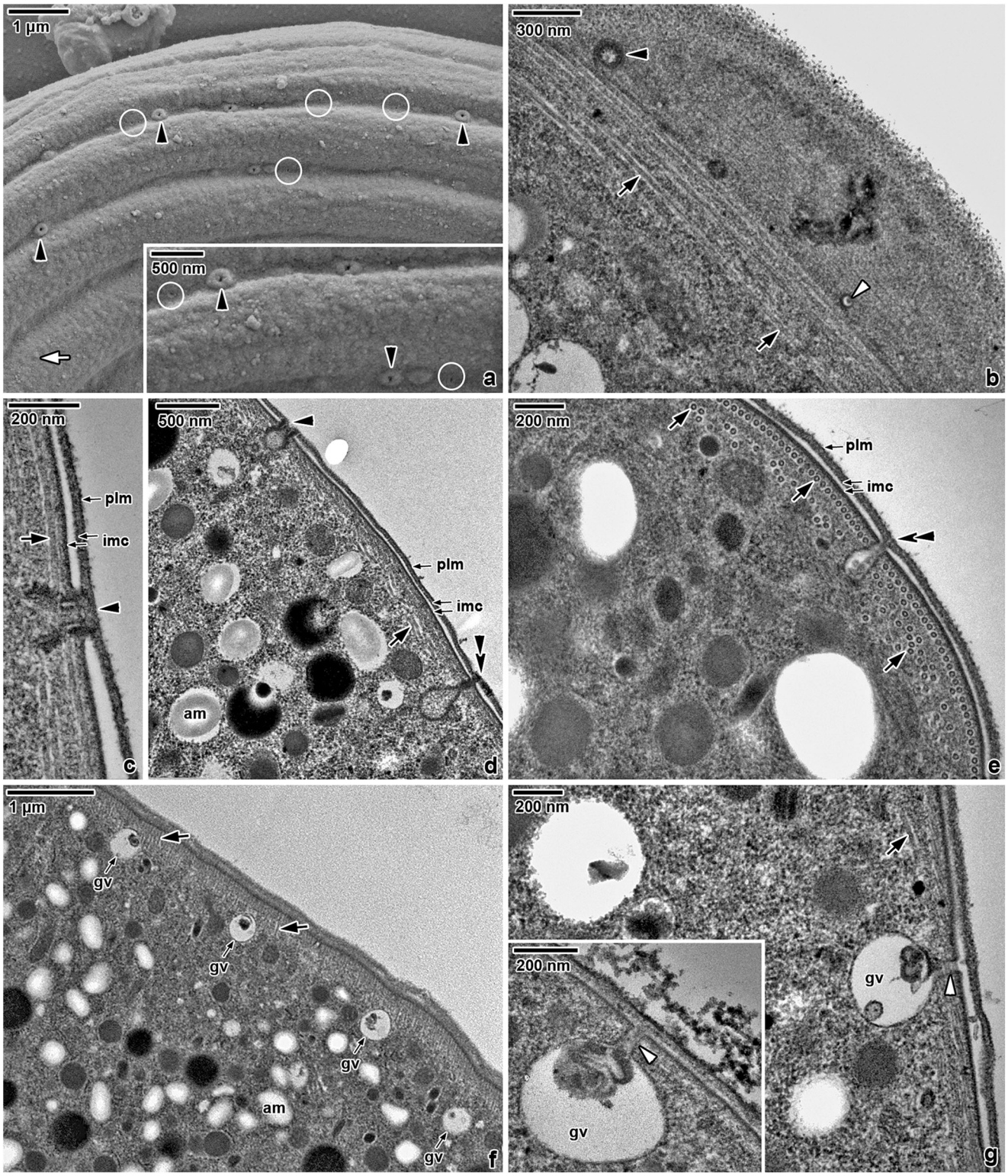

Fig. 2 Micropores and cortical vesicles in *Selenidium pygospionis*. **a** Superficial view of the trophozoite surface comprising the micropores. Inset shows the micropores and holes in the plasma membrane in detail; SEM. **b** Transversally sectioned micropore and duct; TEM. **c**–**e** A detail of pellicle with micropores and drop-shaped vesicles; **c**, **e** TEM; **d** RR TEM. **f** Organisation of the cell cortex and cytoplasm containing globular vesicles distributed regularly in between folds; TEM. **g** Detailed view of globular vesicles crossing the IMC and containing multi-membranous whorls. Inset shows the globular vesicle in detail; RR TEM. am, amylopectin; black arrow, microtubules; black arrowhead, micropore; double black arrowhead, drop-shaped vesicle; gv, globular vesicle; imc, inner membrane complex; plm, plasma membrane; white arrow, folds; white arrowhead, duct connected to vesicular structure; white circle, holes in the plasma membrane

were formed on the folds located at the internal curvature of the bent cell (Fig. 1g). The apical end was organised as a mucron facilitating attachment to the host tissue and nutrition of the parasite. Both the apical and posterior ends were smooth, lacking any folds (Fig. 1f). A single oval nucleus was localised in the middle of the archigregarine cell (Figs. 1a–e, 6a).

The pellicle consisted of a plasma membrane underlain by two cytomembranes forming the inner membrane complex (IMC) (Figs. 1i, j, 2c–e). A thin glycocalyx layer coated the archigregarine surface (Fig. 1j, inset). The cytoplasm was differentiated into a granular endoplasm and subpellicular ectoplasm, the latter containing subpellicular microtubules (21.9 ± 0.1 nm in diameter), micropores, and various vesicular structures (Figs. 1h–j, 2b–g). The outermost set of subpellicular microtubules was continuous, interrupted just beneath the grooves. Additional clusters or single microtubules occurred deeper, beneath the outermost continuous set (Figs. 1i, 2e). An electron-lucent hexagonal sheath (35.3 ± 0.1 nm in diameter) surrounded each microtubule (Fig. 1i). The distance between the two adjacent microtubules was 38 ± 0.3 nm, while the distance between the outermost microtubule set and the internal cytomembrane was, on average, 19.3 ± 0.1 nm. The number of microtubules per 1 μm of pellicle length was 26.6 ± 0.4 in native parasites (controls). Superficial and longitudinal ultrathin sections showed the continuous layer of parallel running microtubules, interrupted only by pores organised in lines (Fig. 1j). The micropores were localised in the grooves between the folds (Figs. 1g, j, 2a) and consisted of a plasma membrane invagination bounded by a collar (Figs. 1j, 2b–d). In addition, numerous drop-shaped vesicles filled with dense particles were connected to the plasma membrane (Fig. 2d, e). Also, globular vesicles containing a coiled lamellar structure (multi-membranous whorls) or dense material were connected by their ducts to the IMC between the folds (Figs. 1j, 2b, f, g). The termination of these vesicles in the IMC measured 43.4 ± 1 nm in diameter and did not reach the plasma membrane. All these micropores and ducts of the vesicles interrupted the otherwise continuous outermost set of subpellicular microtubules (Figs. 1j, 2b–e). Besides classical micropores, additional holes located between the folds and interrupting both the plasma membrane and IMC were observed in several SEM samples. The distance between these holes was, on average, 2167 ± 336 nm (Fig. 2a).

Motility and cytoskeletal organisation in oryzalin- and colchicine-treated *S. pygospionis*

The effect of the disruption of subpellicular microtubules on *S. pygospionis* motility following incubation with microtubule-disrupting/antimitotic agents: 10 and 30 μM oryzalin (acting through the disruption of existing microtubules and blocking the polymerisation of new ones) and 100 mM colchicine (inhibiting microtubules polymerisation by

Table 1 The treatment of living cells of *Selenidium pygospionis* with cytoskeletal drugs

	Drug (concentration)			
Changes/time after drug application	Oryzalin (10 μM)	Colchicine (100 mM)	Jasplakinolide (30 μM)	Cytochalasin D (30 μM)
Initial increase in speed (°compared to control)	≤ 30 min *0.38 ± 0.06 **2.63 ± 1.03	≤ 10 min *0.37 ± 0.02 **2.7 ± 0.21	≥ 5 min *0.38 ± 0.08 **2.6 ± 1.61	–
Decrease in speed to normal, regular movement	≥ 40 min *0.33 ± 0.08 **3.19 ± 1.02	–	≥ 90 min *0.29 ± 0.05 **3.53 ± 0.72	≤ 120 min *0.31 ± 0.06 **3.35 ± 0.65
Further decrease in speed, bending to sides	≥ 160 min *0.19 ± 0.01 **5.24 ± 0.12	≥ 15 min. *0.25 ± 0.06 **4.03 ± 1.32	≥ 150 min *0.20 ± 0.08 **5.18 ± 0.49	≥ 150 min #Still regular movement *0.24 ± 0.03 **4.09 ± 0.5
Decrease in speed, rigidity of posterior 1/3 of cell	–	≤ 30 min.	–	–
Decrease in speed, rigidity of posterior 1/2 of cell	–	≥ 40 min.	–	–
Complete stoppage of motility	≥ 780 min	≥ 90 min	≥ 540 min	≥ 540 min °Only supressed motility
Recovery of motility in the majority of archigregarines after washing in seawater	≥ 5 min	≥ 10 min	≥ 10 min	≥ 10 min

The symbol "–" indicates no obvious changes in the character of motility; "≥" indicates changes appearing after the noted time period; "≤" indicates changes appearing only during the noted time period; "#" indicates observations differing from other trials; "*" indicates beating frequency (beats/s = in Hz equivalent to 1 beat cycle/s, average ± standard error of the mean); "**" indicates beat-to-beat interval (an average time between the two beats in seconds ± standard error of the mean). "°" indicates control archigregarines in seawater continued to move for more than 9 h (the entire experiment duration) with a beating frequency 0.35 ± 0.04 beats/s and beat-to-beat interval of 2.87 ± 0.33 s)

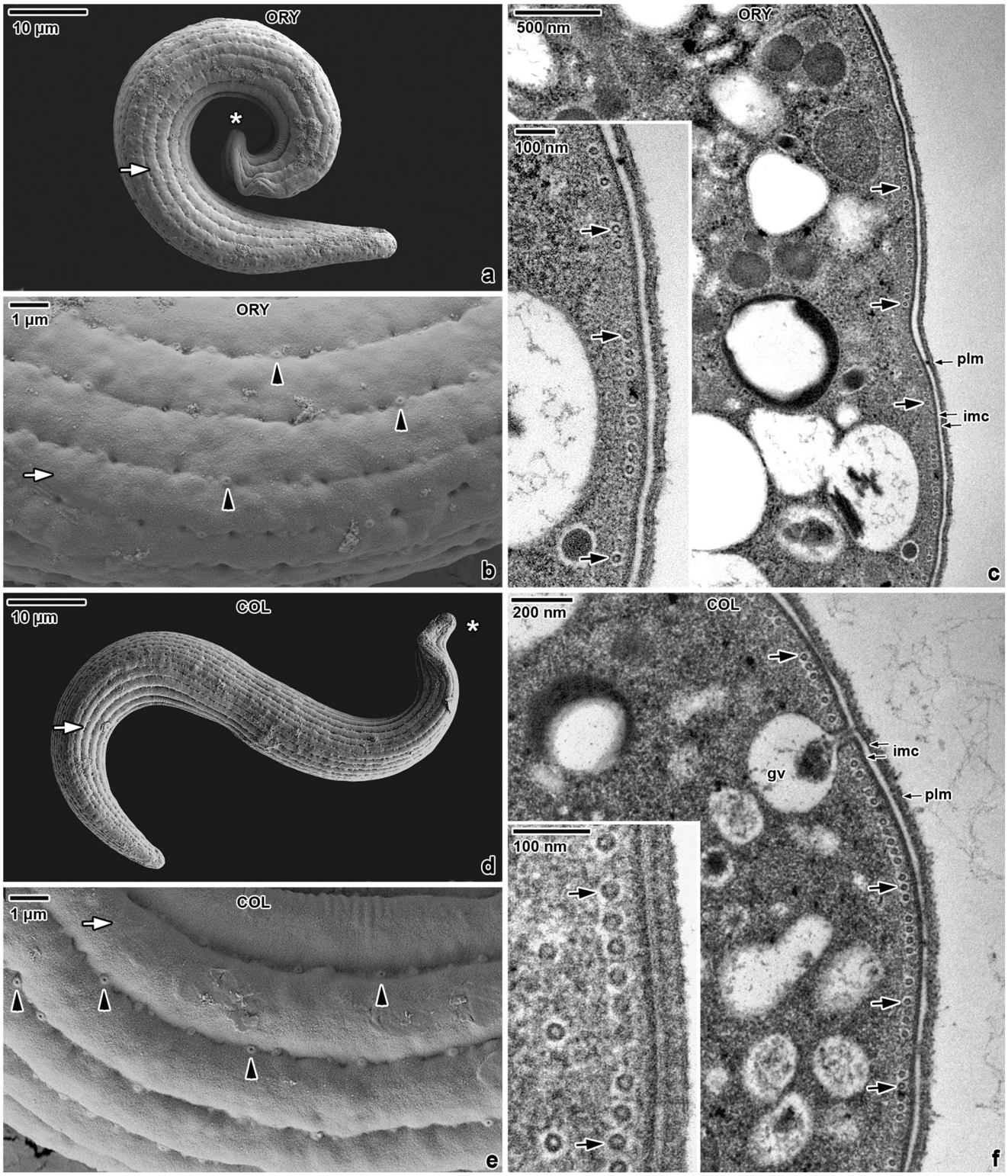

Fig. 3 Organisation of the cell cortex and subpellicular microtubules in *Selenidium pygospionis* after treatment with microtubule-destroying drugs. **a**–**c** Treatment with 10 µm oryzalin for 13 h. **a** A detached archigregarine; SEM. **b** Detail of the surface organisation; SEM. **c** Cross-sectioned cell cortex with subpellicular microtubules. Inset shows the cortex organisation in detail. Note: the outermost layer lacking individual microtubules; TEM. **d**–**f** Treatment with 100 mM colchicine for 90 min. **d** Detached archigregarine; SEM. **e** Detail of the surface organisation; SEM. **f** Cross-sectioned cell cortex with subpellicular microtubules and globular vesicle. Inset shows the organisation of cortex with fading microtubules in detail; TEM. asterisk, apical end; black arrow, microtubules; black arrowhead, micropore; gv, globular vesicle; imc, inner membrane complex; plm, plasma membrane; white arrow, folds

conformational changes through tubulin-colchicine complex) was analysed. High doses of oryzalin (30 μM) had a pronounced effect on archigregarines. Their motility stopped within a period of 40 min, during which the affected parasites exhibited flexures, crampy movements, and the formation of globular cyst-like structures. Some archigregarines did not survive the experiments, as they ruptured. Therefore, oryzalin at a concentration of 10 μM was used for subsequent experimental assays. After some initial increase in movement speed during the first 30 min after drug application, archigregarine motility gradually returned to normal. An additional decrease in motility speed and changes in motility pattern occurred within 160 min of the start of the experiment (Online Resource 2). Experimental assays were stopped after 13 h, when the cessation of motility occurred in the majority of drug-treated *S. pygospionis* cells (Table 1). Colchicine at a concentration of 100 mM caused only a short initial increase in motility speed. Afterwards, movement deceleration followed, together with a rigidity among parasites starting at their posterior end and progressing to the apical tip. Within the first 30 min of the start of the experiment, the last third of the archigregarine cell became rigid, while after 60 min, the posterior half of the cell was already immobile and only the anterior part performed bending from side to side (Online Resource 3). Rigidity progressing to the apical end caused the complete cessation of motility in 90 min, when the experimental assay was stopped (Table 1).

Archigregarines treated with 10 μM oryzalin exhibited fine modifications in pellicle organisation, while the distribution of micropores did not change (Fig. 3a, b). The ultrathin sections revealed interruptions of the normally continuous outermost set of subpellicular microtubules caused by the disappearance of individual microtubules (Fig. 3c). The number of microtubules was reduced to 14.9 ± 1.3 (in 30 μM oryzalin to 8.6 ± 1.4) per 1 μm of the pellicle length. The distance between the two adjacent microtubules in the outermost layer changed to 77.5 ± 5.3 nm on average, and the distance between the IMC and microtubules was 14.4 ± 0.3 nm. While treatment with 100 mM colchicine did not reveal any abnormalities in the pellicle surface under SEM (Fig. 3d, e), the ultrathin cross-sections showed the disappearance and fading of individual microtubules in the subpellicular microtubule sets (Fig. 3f). The number of microtubules in cells incubated with colchicine was 23.1 ± 1.2 per 1 μm of pellicle length. The distance between the two adjacent microtubules in the outermost layer was 42.5 ± 1 nm, and the distance between the IMC and microtubules was 18.7 ± 0.3 nm.

Changes to the subpellicular microtubules were also monitored under a confocal laser scanning microscope (CLSM) in specimens stained with antibody recognising α-tubulin. Phalloidin labelling was used as a control in order to rule out the potential effect of the used drugs (oryzalin and colchicine) on filamentous actin and to verify the impact of microtubule damage on parasite motility. In native (control) archigregarines from filtered seawater, the α-tubulin was arranged in fine longitudinal lines within their cortical region to form a distinct continuous layer, corresponding to the arrangement of subpellicular microtubules (Fig. 4a–c). After treatment with 10 μM oryzalin for 13 h, the subpellicular microtubules degraded and clusters of α-tubulin formed in the ectoplasm (Fig. 4d, e). The same situation occurred after treatment with 30 μM oryzalin (Fig. 4f). Less intense damage to the microtubules was documented in cells treated with 100 mM colchicine for 90 min, where the usually continuous layer of subpellicular microtubules exhibited obvious interruptions (Fig. 4g–i). When compared to oryzalin-treated archigregarines, however, the parallel longitudinal lines in the cortical region were still well preserved and the formation of α-tubulin clusters was less evident.

Fig. 4 The distribution of α-tubulin and F-actin in *Selenidium pygospionis* after treatment with microtubule-destroying drugs. **a**–**c** Controls incubated in seawater. **a** Co-localisation of α-tubulin (FITC) and F-actin (TRITC) in a composite micrograph; CLSM, IFA/phalloidin-TRITC. **b** Localisation of α-tubulin (FITC) in a composite micrograph. Note: the restriction of α-tubulin to the cortical region and its organisation into rows copying the pattern of subpellicular microtubules. Inset shows α-tubulin organisation in detail; CLSM, IFA. **c** Single optical section illustrating the cortical localisation of α-tubulin (FITC) while F-actin (TRITC) is distributed throughout the cytoplasm; CLSM, IFA/phalloidin-TRITC. **d**–**e** Treatment with 10 μm oryzalin for 13 h. **d** Co-localisation of α-tubulin (FITC) and F-actin (TRITC) in a composite micrograph; CLSM, IFA/phalloidin-TRITC. **e** Organisation of α-tubulin (FITC), views of two cells. Note: the clusters of α-tubulin in the cortical region; CLSM, IFA. **f** Treatment with 30 μm oryzalin for 2 h: co-localisation of α-tubulin (FITC) and F-actin (TRITC) in a composite micrograph; CLSM, IFA/phalloidin-TRITC. **g**–**i** Treatment with 100 mM colchicine for 90 min: composite micrograph showing the co-localisation of α-tubulin (FITC) and F-actin (TRITC) (**g**) and organisation of α-tubulin (**h**); CLSM, IFA/phalloidin-TRITC. **i** F-actin (TRITC) distributed throughout the cytoplasm and α-tubulin (FITC) localised in the apical end in a composite view; CLSM, IFA/phalloidin-TRITC. asterisk, apical end; black arrow, microtubules; n, nucleus; white arrow, folds; white arrowhead, clusters of α-tubulin

Motility and cytoskeletal organisation in JAS- and cytochalasin D-treated *S. pygospionis*

The commercially available cytoskeletal probes influencing the polymerisation of actin jasplakinolide (JAS; inducing actin polymerisation and stabilising existing filaments) and cytochalasin D (causing the disruption of actin filaments and inhibiting actin polymerisation) were applied to identify the role of actin filaments in archigregarine motility. Archigregarines treated with 30 μM JAS exhibited regular movements with a slight increase in speed within the first 60 min of drug application. Afterwards, their motility speed gradually decreased to normal. After 150 min, the speed of

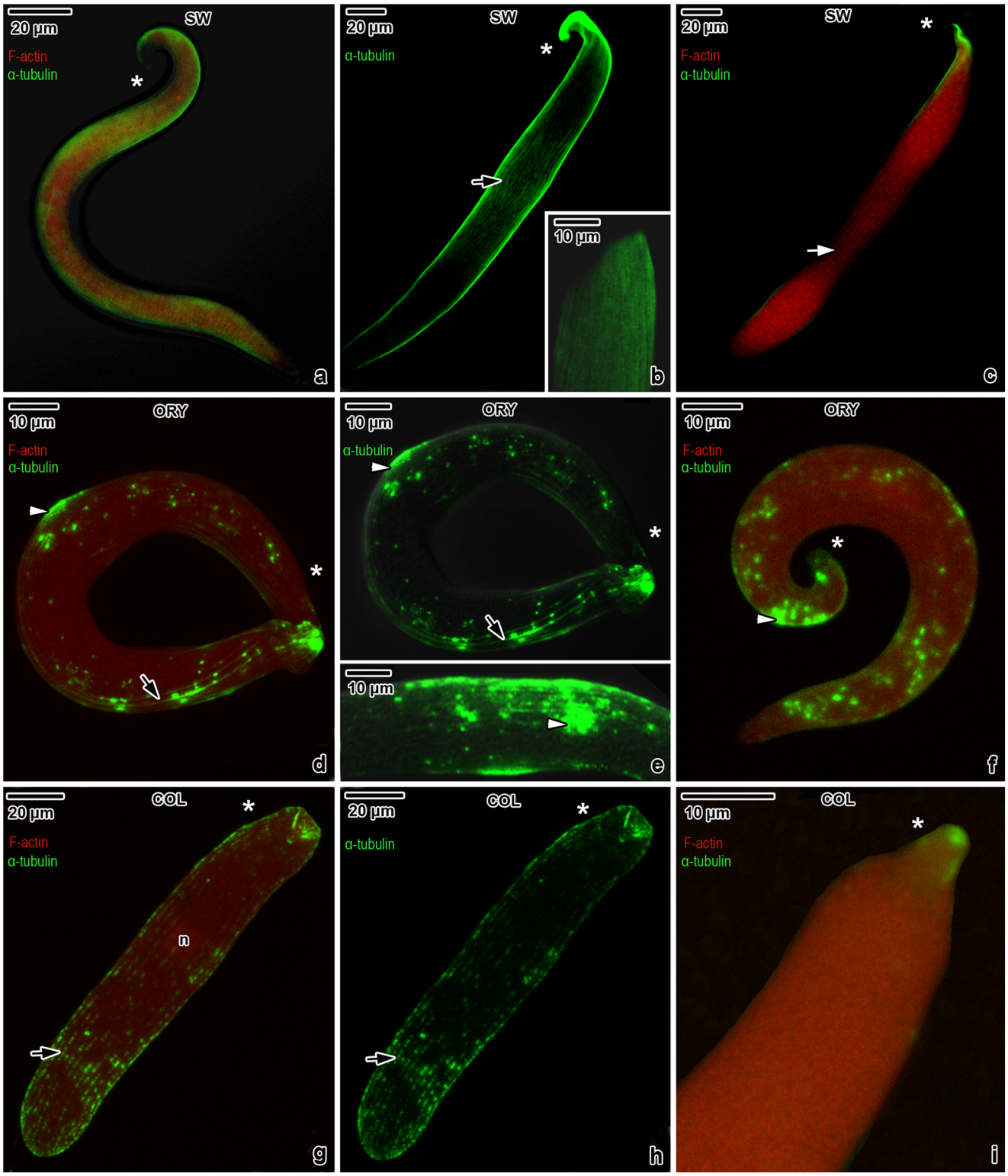

movement continued to decrease continuously, and cells started to twirl and bend to the sides (Online Resource 4). In the majority of JAS-treated archigregarines, motility had ceased after 9 h (Table 1). In contrast, the treatment of parasites with 30 µM cytochalasin D did not induce any visible changes in the pattern of their regular movements, although the speed of their motility decreased during the experiment. After 9 h, the movement was obviously suppressed, though some archigregarines were still motile (Online Resource 5) (Table 1).

SEM analysis of *S. pygospionis* treated with 30 μM JAS revealed a slightly wavy pattern in the pellicle surface (Fig. 5a, b). The ultrathin cross-sections showed the typical organisation of the three-membrane pellicle, without any visible defects. The outermost set of subpellicular microtubules was preserved and remained organised continuously. Individual microtubules were still located within the electron-lucent sheaths and underlying the IMC. Also, deeper localised, irregular clusters of microtubules were preserved (Fig. 5c). In JAS-treated archigregarines, the number of microtubules was 22.6 ± 0.8 per 1 μm of pellicle length, and the distance between the two adjacent microtubules in the outermost layer was 45.8 ± 0.7 nm. The distance between the IMC and microtubules was 19.6 ± 0.3 nm. The incubation of archigregarines with 30 μM cytochalasin D did not result in significant superficial changes to the pellicle (Fig. 5d, e). The ultrathin sections revealed a similar organisation of the cytoskeletal elements to that observed in JAS-treated and control cells, exhibiting the well-preserved characteristic organisation of subpellicular microtubules surrounded by electron-lucent sheaths (Fig. 5f). The number of microtubules in cells incubated with cytochalasin D was 24.6 ± 0.9 per 1 μm of pellicle length. The distance between the two adjacent microtubules in the outermost layer was 43.1 ± 0.6 nm, and the distance between the IMC and microtubules was 16.5 ± 0.4 nm. Similarly, the micropores and vesicles remained in their typical organisation, as described in native archigregarines (Fig. 5b, c, e, f). Longitudinal ultrathin sections confirmed the presence of intact pellicles and microtubules in both treated groups.

The changes in actin organisation after treatment with JAS and cytochalasin D were analysed using direct and indirect (immuno)fluorescent labelling for CLSM. In native (control) archigregarines, indirect immunofluorescent labelling revealed the accumulation of actin into the longitudinal lines copying the pattern of pellicular folds (Fig. 6b, c), while phalloidin labelling revealed a uniform distribution of filamentous actin (F-actin) through the entire cell cytoplasm (Fig. 6b). Phalloidin labelling of *S. pygospionis* affected by 30 μM JAS revealed fluorescence signal multiplication indicating a quantitative increase in actin filaments. An intense signal was also monitored in the position of the nucleus (Fig. 6d, e). The actin, intensively stained with antibody, accumulated in the lines corresponding to the longitudinal pellicular folds. Actin accumulation was also observed in the intracellular axial streak, extending from the middle of the anterior end to the posterior end and forming a ring around the nucleus (Fig. 6e, f). In contrast, the fluorescent signal of actin labelled in cytochalasin D-treated archigregarines was very weak and lacked its specific organisational pattern (Fig. 6g–j).

Discussion

Pellicle organisation and pore distribution in *Selenidium* archigregarines

The entire surface of *S. pygospionis* is covered by glycocalyx and folded into 22–30 (usually 28) broad and low folds separated by grooves with micropores (Paskerova et al. 2018). The micropores were suggested to have a feeding function in some gregarine groups; however, typical archigregarine myzocytotic feeding is considered to be associated with the apically located mucron (Desportes and Schrével 2013; Paskerova et al. 2018; Schrével 1971a; Schrével et al. 2016; Simdyanov and Kuvardina 2007; Wakeman and Horiguchi 2017). In *S. melongena* and *S. serpulae*, micropores were shown to lead to the pinocytotic whorled vesicles (Leander 2007; Wakeman et al. 2014). In contrast, in *S. pygospionis*, the vesicular structures connected to the micropores were translucent and appeared empty. Instead, the whorled material was observed in the ectoplasmic globular vesicles. When comparing the control and drug-treated *S. pygospionis* cells, the presence, distribution, and sizes of the micropores were unchanged. Similarly, the globular and drop-shaped cytoplasmic vesicles comprising some dense material or multimembranous whorls, located between the folds and inserted with their terminations to the pellicle, remained unaffected by the drugs. These vesicular structures, already found in several *Selenidium* species, were suggested to have an additional role in surface-mediated nutrition (Paskerova et al. 2018; Schrével et al. 2016; Wakeman and Horiguchi 2017).

Motility and cytoskeleton organisation in native *Selenidium* archigregarines

Mature parasites of *Selenidium* spp. have a cell organisation similar to invasive apicomplexan zoites (Schrével and Desportes 2015). The typical apicomplexan pellicle covering *Selenidium* representatives is folded and underlain by layers of microtubules. Their apical end—the mucron (dedicated for myzocytosis)—comprises the conoid, rhoprties, and micronemes (Paskerova et al. 2018; Schrével and Desportes 2015). These plesiomorphic characteristics place archigregarines as the most representatives of ancestral gregarines (Schrével 1971a; Schrével and Desportes 2015; Leander 2008). Trophozoites and gamonts of *Selenidium pygospionis* performed a bending motility with a coiling of their anterior end. Specifically, their motility was generated only in one cell plane, while other *Selenidium* species can bend in different cell planes (Paskerova et al. 2018). A variety of other movements have been observed in detached archigregarines of the family Selenidiidae, sometimes in combination with bending motility, e.g. pendular motility in *S. pendula* and *S. orientale*, rolling and coiling movements

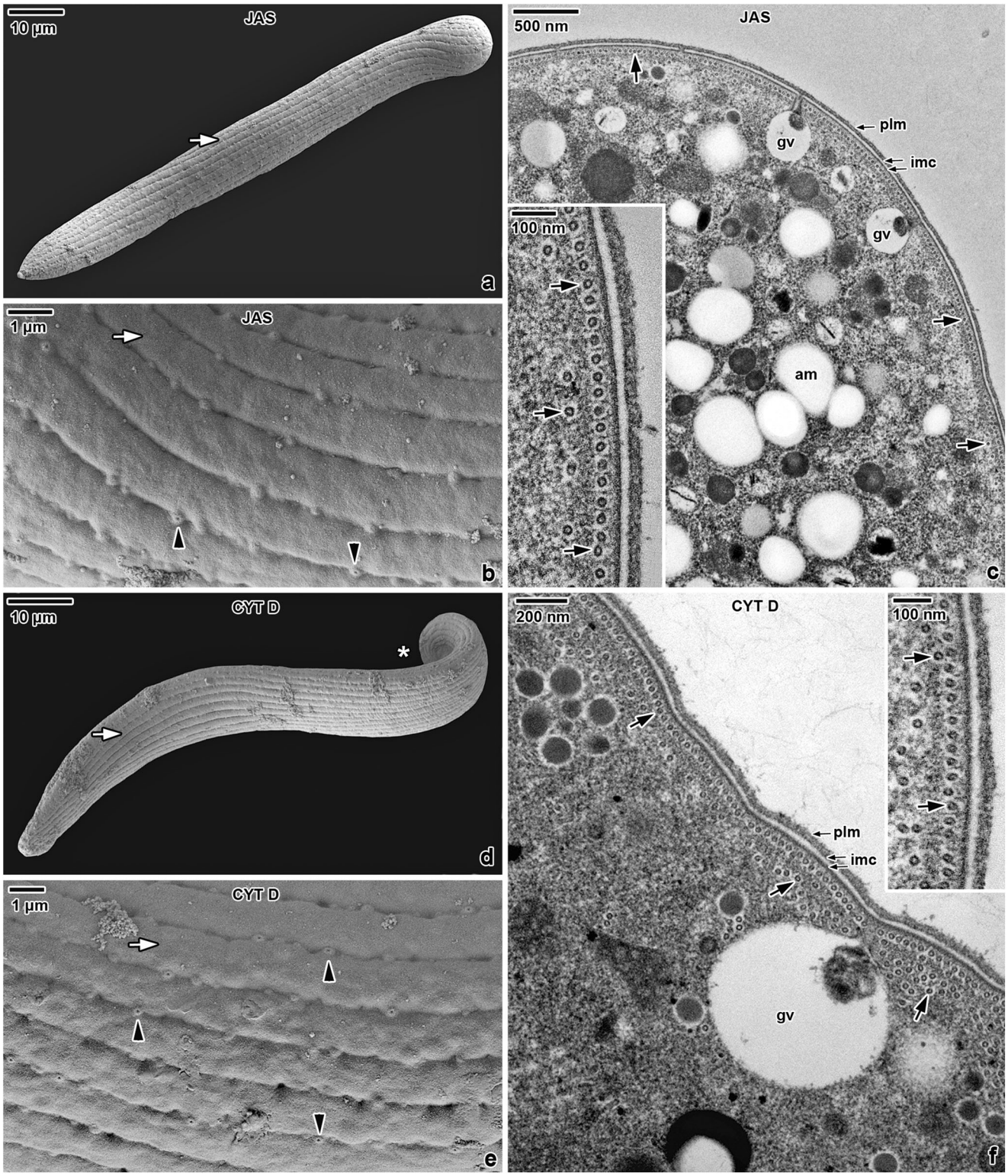

Fig. 5 Organisation of the cortex in *Selenidium pygospionis* after treatment with actin-modifying drugs. **a**–**c** Treatment with 30 µm JAS for 9 h. **a** Detached archigregarine; SEM. **b** Detail of the surface organisation; SEM. **c** Cross-sectioned cell cortex with subpellicular microtubules and vesicles. Inset shows the organisation of the cortex in detail; TEM. **d**–**f** Treatment with 30 µm cytochalasin D for 9 h. **d** Detached trophozoites; SEM. **e** Detail of the surface organisation; SEM. **f** Cross-sectioned cell cortex with subpellicular microtubules and globular vesicle. Inset shows the organisation of the cortex in detail; TEM. am, amylopectin; asterisk, apical end; black arrow, microtubules; black arrowhead, micropore; gv, globular vesicle; imc, inner membrane complex; plm, plasma membrane; white arrow, folds

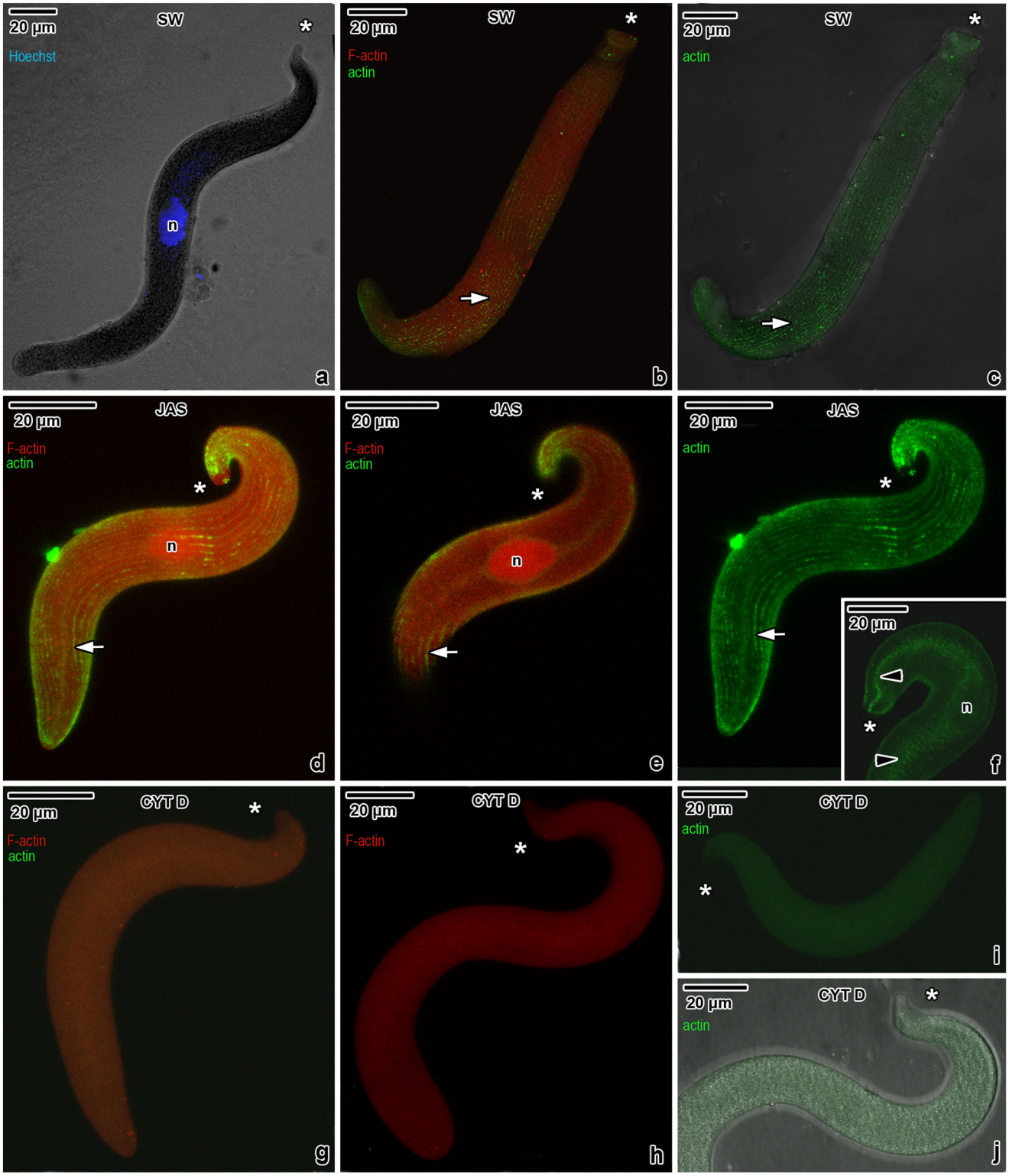

in *S. sabellariae* and *S. hollandei*, twisting movements in *S. terebellae*, and twisting and contracting movements in *S. serpulae* (Desportes and Schrével 2013; Leander et al. 2003; Leander 2007; Rueckert and Horák 2017; Schrével and Desportes 2015; Schrével et al. 2016; Simdyanov and Kuvardina 2007; Wakeman et al. 2014). Slow-motion whip-like movements (the propagation of bending waves) in attached trophozoites and coiling movements in detached

◀ **Fig. 6** Actin distribution in *Selenidium pygospionis* after treatment with actin-modifying drugs. **a**–**c** Controls incubated in seawater. **a** Composite micrograph showing the localisation of the nucleus stained with Hoechst; CLSM in combination with transmission light. Composite view showing the co-localisation of actin (FITC) and F-actin (TRITC) (**b**), and localisation of actin (FITC) (**c**); CLSM (**b**) and CLSM in combination with transmission light (**c**), IFA/phalloidin-TRITC. **d**–**f** Treatment with 30 μm JAS for 9 h. Co-localisation of actin (FITC) and F-actin (TRITC) in a composite micrograph (**d**) and a series of optical sections from the middle region of the cell (**e**); CLSM, IFA/phalloidin-TRITC. **f** Composite micrograph visualising actin (FITC) organisation. Inset shows accumulation of actin in the position of the axial streak and around the nucleus on selected optical sections; CLSM, IFA. **g**–**j** Treatment with 30 μm cytochalasin D for 9 h. **g** Co-localisation of actin (FITC) and F-actin (TRITC) in a composite micrograph; CLSM, IFA/phalloidin-TRITC. **h** Micrograph composed of all optical sections showing the organisation and localisation of F-actin (TRITC); CLSM, phalloidin-TRITC. **i**, **j** Composite micrographs showing the localisation of actin (FITC); CLSM (**i**) and CLSM in a combination with transmission light (**j**), IFA. asterisk, apical end; black arrowhead, axial streak; n, nucleus; white arrow, folds

parasites were observed in *S. fallax* and were preceded by a slight longitudinal contraction (Mellor and Stebbings 1980; Stebbings et al. 1974). The bending/rolling/pendular motility of *Selenidium* spp. is similar to that found in apicomplexan sporozoites (Leander 2008) and blastogregarines (Valigurová et al. 2017). The performance of cell movement enables archigregarines to find syzygy partners, invade adjacent epithelial cells, and move nutrients across their cell surface within the intestinal lumen (Leander 2007).

In apicomplexan zoites, the subpellicular microtubules have a characteristic organisation and length; they are nucleated from the apical polar ring (a unique microtubule organising centre (MTOC)) and end in the region behind the nucleus (Morrissette and Sibley 2002a, b). In contrast, in the blastogregarine *S. nematoides* and archigregarines, the microtubules run throughout the entire body length (Schrével et al. 2016; Simdyanov and Kuvardina 2007; Valigurová et al. 2017; Wakeman et al. 2014; Wakeman and Horiguchi 2017). A mechanism based on the cooperation between the archigregarine pellicle (IMC) and longitudinally oriented subpellicular microtubules, acting like an analogue of the musculocuticular system of nematodes, was proposed for archigregarine motility (Leander 2007; Paskerova et al. 2018; Stebbings et al. 1974). Meanwhile, the sliding of microtubules provided by microtubule-associated molecular motors (MAPs) such as kinesins and dyneins, comparable to the system occurring in a ciliary axoneme, was suggested as the mechanism for the propagation of bending waves in *Selenidium* spp. (Mellor and Stebbings 1980; Stebbings et al. 1974). Each microtubule is surrounded by an electron-transparent sheath likely playing an important role in microtubular sliding (Leander 2007; Mellor and Stebbings 1980; Stebbings et al. 1974). The association between the mitochondria (providing chemical energy in ATP for MAPs activity) and subpellicular microtubules is necessary to ensure functional cell motility (Leander 2006; Mellor and Stebbings 1980; Schrével 1971b). The ectoplasm of actively motile Selenidiidae representatives comprise a higher number of subpellicular microtubules compared to slow-moving species, and their mitochondria are concentrated in the cortical zone under the microtubules (Schrével 1971b; Simdyanov and Kuvardina 2007). As evidence of this, the immotile species *S. melongena* lacks an assembly of subpellicular microtubules (Wakeman et al. 2014). The positive correlation between active motility and a high number of mitochondria arranged beneath the subpellicular microtubules is supported by ultrastructural observations of the archigregarine *S. pygospionis* (Paskerova et al. 2018) and the blastogregarine *S. nematoides* (Valigurová et al. 2017). The movement speed of *Selenidium* species was further suggested to be related to oxygen availability in their environments (Schrével 1971a). In addition, the involvement of the axial streak together with putative microfilaments was suggested to participate in archigregarine motility (Fowell 1936; Paskerova et al. 2018).

The subpellicular microtubules organised in several layers were also suggested to be the leading motor structure in the movement of the blastogregarine *Siedleckia nematoides* (genus *Siedleckia* is comparable with *Selenidium* archigregarines due to the similarities in external morphology and movement patterns), which performs pendular, twisting, and undulating movements (Caullery and Mesnil 1898; Simdyanov et al. 2018; Valigurová et al. 2017).

Cytoskeletal drug-induced motility and cytoskeleton organisation in *Selenidium* archigregarines

The so-called glideosome concept, proposed for apicomplexan zoites, describes an actomyosin motor localised between the parasite plasma membrane and the IMC and connected to the transmembrane adhesin complexes contacting the substrate. This motor requires a stable subpellicular network of microtubules, connected through intramembranous particles to the IMC (Dubremetz et al. 1998; Kappe et al. 2004; Keeley and Soldati 2004; Matuschewski and Schüler 2008; Opitz and Soldati 2002). The subpellicular microtubules of apicomplexans are unusually stable and withstand high pressure, cold, and various detergents (Morrissette and Sibley 2002a; Morrissette et al. 1997). It is known that oryzalin and colchicine destroy subpellicular microtubules in *T. gondii* tachyzoites (Morrissette and Sibley 2002b; Stokkermans et al. 1996). Only at a high colchicine concentration (1 mM) shortening of the microtubules was observed. The microtubules were, however, markedly sensitive to oryzalin and were absent in oryzalin-treated parasites (de Souza and Attias 2010; Stokkermans et al. 1996; Valigurová et al. 2017). Drug-treated replicative stages of apicomplexans lacking subpellicular microtubules are non-polar, non-motile,

and non-invasive (Stokkermans et al. 1996). Compared to apicomplexan zoites, blastogregarine *S. nematoides* (Valigurová et al. 2017) and archigregarines seem to be more tolerant of microtubule-depolymerising drugs at high concentrations.

Previous studies testified to the role of subpellicular microtubules in the motility of archigregarines by using colchicine to block the assembly of microtubules subunits and urea to induce the depolymerisation of microtubules (Schrével et al. 1974; Stebbings et al. 1974). The cessation of bending movements in *S. fallax* attached trophozoites were detected after the application of various colchicine concentrations (0.1–2%) (Stebbings et al. 1974). In treated archigregarines, the number of microtubules was significantly reduced and the remaining microtubules appeared to be destroyed. In addition, the pattern of pellicular folding was altered compared to native parasites. According to the colchicine concentration, the duration of parasite motility varied from 19 to 360 min (Stebbings et al. 1974). Similarly, after the incubation of *S. hollandei* trophozoites in seawater containing 0.6–1.0 M urea for 1 h, the depolymerisation of subpellicular microtubules occurred and the rolling motility stopped. In trophozoites returned to seawater, motility was restored and microtubule polymerisation regressed (Desportes and Schrével 2013; Schrével et al. 1974). In *S. pygospionis*, the cessation of motility was observed after 90 min of exposure to 100 mM colchicine. Similarly to the observations on *S. nematoides* (Valigurová et al. 2017), the rigidity of the cell proceeded from the posterior to anterior end until motility stopped. In colchicine-treated *S. pygospionis* in our study, the microtubules seemed to fade so that, in the ultrathin sections, their borders became indistinct. The empty regions were observed in the commonly continuous outermost microtubular layer; however, the number of microtubules differed only moderately from controls. Sometimes, remnants of microtubules were still preserved in the subpellicular layer. Archigregarines treated with 10 μM oryzalin moved for 13 h until their bending motility stopped. Empty spaces in the outermost microtubular layer in oryzalin-treated archigregarines resulted in a significant reduction of a number of microtubules per 1 μm of pellicle length. The degradation of microtubules in the inner second and/or third layers was also observed. Similar observations were documented in blastogregarines; while in oryzalin-treated *S. nematoides*, the microtubules gradually faded away, in those treated in colchicine, they completely disappeared in some regions (Valigurová et al. 2017). In comparison with *S. pygospionis*, blastogregarines seem to have even greater tolerance to oryzalin in high concentrations, and both drugs appear to influence the microtubule depolymerisation in different manner (i.e. in oryzalin-treated *S. pygospionis* individual microtubules completely disappeared from the outermost layer, while in *S. nematoides*, they rather gradually faded). The different stabilities of microtubules could be the result of the influence of associated proteins or proteins that specifically interact with only one of microtubule populations (Morrissette and Sibley 2002b). These proteins may represent important co-factors modulating the effects of individual drugs (Fromes et al. 1996).

In native cells of *S. pygospionis* α-tubulin was restricted to the cortical region and organised in longitudinal lines corresponding to the subpellicular microtubules; this is similar to *S. terebella* archigregarines in which α-tubulin was localised in the mucron region and below the cell surface in a pattern corresponding to the microtubules (Wakeman et al. 2014). The α-tubulin staining of colchicine-treated *S. pygospionis* revealed the preservation of the longitudinal arrangement of microtubules, but these were destroyed (the lines were interrupted) and small tubulin clusters had formed. In oryzalin-treated archigregarines, the complete destruction of microtubules occurred and distinct α-tubulin clusters were clearly seen. While both drugs (colchicine and oryzalin) blocked the motility, the differences were observed in how the drugs acted and in the cellular changes in *S. pygospionis* observed during ultrastructural and fluorescence analyses. These different effects of the applied drugs on subpellicular microtubules in *S. pygospionis* cells could be explained by the presence and regulatory capacity of associated proteins.

Actin, as a part of the actomyosin motor, is considered to be essential for gliding and host cell invasion in apicomplexan zoites (Opitz and Soldati 2002). Apicomplexan actin filaments are thought to be exceedingly transient, and their observation is possible only after treatment with an actin-stabilising drug such as JAS (Morrissette and Sibley 2002a; Schmitz et al. 2010). The majority of actin is presented in a globular form in *T. gondii* (Dobrowolski et al. 1997) or in short filaments, dimers, or monomers in *Plasmodium* parasites (Kumpula et al. 2017; Schmitz et al. 2005). In *P. berghei* and *T. gondii*, the JAS-induced increase in F-actin concentration resulted in fast-moving zoites, indicating that actin filaments are rate limiting (Münter et al. 2009; Wetzel et al. 2003). Treatment with cytochalasin D, however, led to increased adhesion dynamics and inhibited the invasion and motility of parasites (Dobrowolski and Sibley 1996; Münter et al. 2009).

The incubation of *S. pygospionis* with actin-modifying drugs revealed its tolerance to these drugs at relatively high concentrations. The movement of JAS-treated archigregarines ceased in most individuals after 9 h, while cytochalasin D suppressed motility but did not stop it. The inhibition of pendular movement in *S. pendula* by cytochalasin B was observed by Ghazali and Schrével (1995). However, cytochalasin D specifically binds to the actin filaments in contrast to cytochalasin B, which binds to both the actin filaments and glucose transporters, and therefore, motility could be blocked by several mechanisms (Cooper 1987). On the basis of our experiments with *S. pygospionis*, where obvious changes in motility and its blocking occurred along with an increase in

actin filaments, we conclude that F-actin serves rather as a supportive component for subpellicular microtubules. A previous study concluded that the presence of actin and myosin along with the cytochalasin B-induced inhibition of movement suggests that the actomyosin system could provide the necessary force for the pendular and rolling motility in *Selenidium* together with microtubule-membrane interactions (Ghazali and Schrével 1995). Support for this theory can be found also in a study on *S. nematoides*, which revealed cross-linking protein complexes, presumably of an actin nature, consisting of proteins embedded in the IMC and the network around subpellicular microtubules, which appeared to anchor the microtubules to the IMC (Valigurová et al. 2017). These protein complexes were found to influence microtubule spacing in S. *nematoides* treated with actin-modifying drugs, and polymerised form of these proteins seemed to be essential for parasite motility (Valigurová et al. 2017). Observations in Valigurová et al. (2017) confirmed that the motility of blastogregarines differs from the glideosome concept proposed for apicomplexans zoites. Nevertheless, it should be noted that the glideosome concept needs to be revaluated, as previous studies have shown that motility can be preserved after the knocking out of several key proteins associated with glideosome function (e.g. actin, myosin, or microneme proteins) (Egarter et al. 2014; Tardieux and Baum 2016; Whitelaw et al. 2017). While motility and actin organisation/accumulation in *S. pygospionis* individuals was also affected by the treatment with JAS and cytochalasin D, no significant changes occurred in the position of the subpellicular microtubules or in the distance between the outermost microtubule set and the internal cytomembrane.

Conclusions

Our study, based on experimental assays employing cytoskeletal drugs to influence the polymerisation of the two main cytoskeletal components, actin and tubulin, and evaluated using a combined approach involving light, electron, and confocal microscopy confirmed the two main elements responsible for bending motility in *S. pygospionis*. The main motor structure appears to be constituted by the subpellicular microtubules. The cessation of motility (the rigidity of archigregarines) in colchicine-treated cells proceeded gradually along the archigregarine, starting at the posterior end and progressing to the apical one. This observation suggests that microtubule depolymerisation begins in the caudal region and continues towards the apical polar ring (MTOC; the structure where microtubules initially originated). The experiments with actin-modifying drugs demonstrated the role of actin in *S. pygospionis* motility, indicating it to have a mostly function as a supportive component for subpellicular microtubules. Despite the morphological similarity of archigregarine trophozoites (considered to be overgrown apicomplexan zoites = hypersporozoites) to apicomplexan zoites, the bending motility of *S. pygospionis* differs from substrate-dependent gliding motility in *Toxoplasma* or *Plasmodium* invasive stages (Håkansson et al. 1999; Münter et al. 2009). We believe that this bending motility predominates and possibly replaces substrate-dependent gliding during archigregarine development from zoite to trophozoite stages. Within Apicomplexa, the bending movement performed by archigregarines is most similar to that observed in the blastogregarine *S. nematoides* (Valigurová et al. 2017). In both groups, parasites continued to bend even after the detachment from the host tissue, and their unique movement, therefore, cannot be described as substrate-dependent.

Acknowledgements Financial support for MK, AV, and AD was provided by the Czech Science Foundation, project No. GBP505/12/G112 (ECIP - Centre of excellence). NV received financial support from MEYS CR (LO1212) and EC (CZ.1.05/2.1.00/01.0017); GGP, from St. Petersburg State University (Grants 1.42.1493.2015, 1.42.1099.2016, project 109-9017); GGP and TGS, from the Russian Foundation for Basic Research (Grant 18-04-00324). We are grateful to Prof. Dominique Soldati-Favre (University of Geneva) for providing the monoclonal anti-actin antibody.

Compliance with ethical standards

Conflict of interests The authors declare that they have no conflict of interest.

Abbreviations CLSM, confocal laser scanning microscopy; COL, colchicine; CYT D, cytochalasin D; DMSO, dimethyl sulfoxide; FITC, fluorescein isothiocyanate; IFA, indirect immunofluorescent assay; IMC, inner membrane complex; JAS, jasplakinolide; LM, light microscopy; ORY, oryzalin; PBS, phosphate-buffered saline; PFA, 4% paraformaldehyde; RR, ruthenium red; SEM, scanning electron microscopy; SW, seawater; TEM, transmission electron microscopy; TRITC, tetramethylrhodamine isothiocyanate

References

Caullery M, Mesnil F (1898) Sur un Sporozoaire aberrant (*Siedleckia* n. g.). C R Soc Biol 5:1093–1095

Cooper JA (1987) Effects of cytochalasin and phalloidin on actin. J Cell Biol 105 (4):1473–1478. https//doi.org/https://doi.org/10.1101/SQB.1973.037.01.069

De Souza W, Attias M (2010) Subpellicular microtubules in Apicomplexa and Trypanosomatids. In: de Souza W (ed) Structures and organelles in pathogenic protists. Springer-Verlag, Berlin, Heidelberg, pp 27–62. https://doi.org/10.1007/978-3-642-12863-9

Desportes I, Schrével J (2013) The gregarines, the early branching Apicomplexa (2 vols). Treatise on zoology - anatomy, taxonomy, biology. BRILL, Leiden – the Netherlands. 781 pp

Dobrowolski JM, Sibley LD (1996) *Toxoplasma* invasion of mammalian cells is powered by the actin cytoskeleton of the parasite. Cell 84 (6): 933–939. https://doi.org/10.1016/S0092-8674(00)81071-5

Dobrowolski JM, Niesman IR, Sibley LD (1997) Actin in the parasite *Toxoplasma gondii* is encoded by a single copy gene, act1 and exists

primarily in a globular form. Cell Motil Cytoskeleton 37 (3):253–262. https://doi.org/10.1002/(SICI)1097-0169(1997)37:3<253::AID-CM7>3.0.CO;2-7

Dubremetz JF, Garcia-Réguet N, Conseil V, Fourmaux MN (1998) Apical organelles and host-cell invasion by Apicomplexa. Int J Parasitol 28 (7):1007–1013. https://doi.org/10.1016/S0020-7519(98)00076-9

Egarter S, Andenmatten N, Jackson AJ, Whitelaw JA, Pall G, Black JA, Ferguson DJ, Tardieux I, Mogilner A, Meissner M (2014) The *Toxoplasma* acto-myoA motor complex is important but not essential for gliding motility and host cell invasion. PLoS One 9(3): e91819. https://doi.org/10.1371/journal.pone.0091819

Fowell RR (1936) The fibrillar structures of Protozoa, with special reference to schizogregarines of the genus *Selenidium*. J R Micr Soc 56: 12–28

Fromes Y, Gounon P, Veitia R, Bissery MC, Fellous A (1996) Influence of microtubule-associated proteins on the differential-effects of paclitaxel and docetaxel. J Protein Chem 15(4):377–388

Ghazali M, Schrével J (1993) Myosin like protein (M_r 175,000) in *Gregarina blaberae*. J Eukaryot Microbiol 40(3):345–354

Ghazali M, Schrével J (1995) Identification and localization of proteins in gregarines that are immunologically related to smooth muscle α-actinin. Eur J Protistol 31 (3):292–301. https://doi.org/10.1016/S0932-4739(11)80093-3

Ghazali M, Philippe M, Deguercy A, Gounon P, Gallo J, Schrével J (1989) Actin and spectrin-like (M_r= 260-240 000) proteins in gregarines. Biol Cell 67(2):173–184. https://doi.org/10.1111/j.1768-322X.1989.tb00860.x

Håkansson S, Morisaki H, Heuser J, Sibley LD (1999) Time-lapse video microscopy of gliding motility in *Toxoplasma gondii* reveals a novel, biphasic mechanism of cell locomotion. Mol Biol Cell 10(11): 3539–3547. https://doi.org/10.1091/mbc.10.11.3539

Heintzelman MB (2004) Actin and myosin in *Gregarina polymorpha*. Cell Motil Cytoskeleton 58(2):83–95. https://doi.org/10.1002/cm.10178

Heintzelman MB, Mateer MJ (2008) GpMyoF, a WD40 repeat-containing myosin associated with the myonemes of *Gregarina polymorpha*. J Parasitol 94(1):158–168. https://doi.org/10.1645/GE-1339.1

Kappe SH, Buscaglia C, Bergman LW, Coppens I, Nussenzweig V (2004) Apicomplexan gliding motility and host cell invasion: overhauling the motor model. Trends Parasitol 20(1):13–16. https://doi.org/10.1016/j.pt.2003.10.011

Keeley A, Soldati D (2004) The glideosome a molecular machine powering motility and host-cell invasion by Apicomplexa. Trends Cell Biol 14(10):525–528. https://doi.org/10.1016/j.tcb.2004.08.002

Kováčiková M, Vaškovicová N, Nebesářová J, Valigurová A (2018) Effect of jasplakinolide and cytochalasin D on cortical elements involved in the gliding motility of the eugregarine *Gregarina garnhami* (Apicomplexa). Eur J Protistol 66:97–114. https://doi.org/10.1016/j.ejop.2018.08.006

Kumpula EP, Pires I, Lasiwa D, Piirainen H, Bergmann U, Vahokoski J, Kursula I (2017) Apicomplexan actin polymerization depends on nucleation. Sci Rep 7(12137):1–10. https://doi.org/10.1038/s41598-017-11330-w

Leander BS (2006) Ultrastructure of the archigregarine *Selenidium vivax* (Apicomplexa) – a dynamic parasite of sipunculid worms (host: *Phascolosoma agassizii*). Mar Biol Res 2(3):178–190. https://doi.org/10.1080/17451000600724395

Leander BS (2007) Molecular phylogeny and ultrastructure of *Selenidium serpulae* (Apicomplexa, Archigregarinia) from the calcareous tubeworm *Serpula vermicularis* (Annelida, Polychaeta, Sabellida). Zool Scripta 36(2):213–227. https://doi.org/10.1111/j.1463-6409.2007.00272.x

Leander BS (2008) Marine gregarines: evolutionary prelude to the apicomplexan radiation? Trends Parasitol 24(2):60–67. https://doi.org/10.1016/j.pt.2007.11.005

Leander BS, Harper JT, Keeling PJ (2003) Molecular phylogeny and surface morphology of marine aseptate gregarines (Apicomplexa) *Selenidium* spp. and *Lecudina* spp. J Parasitol 89(6):1191–1205. https://doi.org/10.1645/GE-3155

Matuschewski K, Schüler H (2008) Actin/myosin-based gliding motility in apicomplexan parasites. In: Burleigh BA, Soldati-Favre D (eds) Molecular mechanisms of parasite invasion, Subcell Biochem, vol 47. Springer, New York, NY, pp 110–120. https://doi.org/10.1007/978-0-387-78267-6_9

Mellor JS, Stebbings H (1980) Microtubules and the propagation of bending waves by the archigregarine, *Selenidium fallax*. J Exp Biol 87:149–161

Morrissette NS, Sibley LD (2002a) Cytoskeleton of apicomplexan parasites. Microbiol Mol Biol Rev 66(1):21–38. https://doi.org/10.1128/MMBR.66.1.21-38.2002

Morrissette NS, Sibley D (2002b) Disruption of microtubules uncouples budding and nuclear division in *Toxoplasma gondii*. J Cell Sci 115(5):1017–1025

Morrissette NS, Murray JM, Roos DS (1997) Subpellicular microtubules associate with an intramembranous particle lattice in the protozoan parasite *Toxoplasma gondii*. J Cell Sci 110:35–42

Münter S, Sabass B, Selhuber-Unkel C, Kudryashev M, Hegge S, Engel U, Spatz JP, Matuschewski K, Schwarz US, Frischknecht F (2009) *Plasmodium* sporozoite motility is modulated by the turnover of discrete adhesion sites. Cell Host Microbe 6(6):551–562. https://doi.org/10.1016/j.chom.2009.11.007

Opitz C, Soldati D (2002) The glideosome: a dynamic complex powering gliding motion and host cell invasion by *Toxoplasma gondii*. Mol Microbiol 45(3):597–604. https://doi.org/10.1046/j.1365-2958.2002.03056.x

Paskerova GG, Miroliubova TS, Diakin A, Kováčiková M, Valigurová A, Gillou L, Aleoshin VV, Simdyanov TG (2018) Fine structure and molecular phylogeny of two marine gregarines, *Selenidium pygospionis* n. sp. and *S. pherusae* n. sp., with notes on the phylogeny of Archigregarinida (Apicomplexa). Protist 169(6):826–852. https://doi.org/10.1016/j.protis.2018.06.004

Rueckert S, Horák A (2017) Archigregarines of the english channel revisited: new molecular data on *Selenidium* species including early described and new species and the uncertainties of phylogenetic relationships. PLoS One 12(11):e0187430. https://doi.org/10.1371/journal.pone.0187430

Schmitz S, Grainger M, Howell S, Calder LJ, Gaeb M, Pinder JC, Holder AA, Veigel C (2005) Malaria parasite actin filaments are very short. J Mol Biol 349(1):113–125. https://doi.org/10.1016/j.jmb.2005.03.056

Schmitz S, Schaap IA, Kleinjung J, Harder S, Grainger M, Calder L, Rosenthal PB, Holder AA, Veigel C (2010) Malaria parasite actin polymerization and filament structure. J Biol Chem 285(47):36577–36585. https://doi.org/10.1074/jbc.M110.142638

Schrével J (1971a) Observations biologiques et ultrastructurales sur les Selenidiidae et leurs conséquences sur la systématique des Grégarinomorphes. J Protozool 18(3):448–470

Schrével J (1971b) Contribution à l'étude des Selenidiidae parasites d'annélides polychètes. II Ultrastructure de quelques trophozoïtes. Protistologica 7:101–130

Schrével J, Desportes I (2015) Gregarines. In: Mehlhorn H (ed) Encyclopedia of parasitology. Springer-Verlag, Berlin, Heidelberg, 47 pp

Schrével J, Philippe M (1993) The gregarines. In: Kreier JP, Baker JR (ed) Parasitic protozoa. 2nd edition. Academic Press, pp 133-245

Schrével J, Buissonnets S, Metais M (1974) Action de l'urée sur la motilité et les microtubules sous pelliculaires du protozoaire *Selenidium hollandei*. C R Acad Sci Paris 278:2201–2204

Schrével J, Valigurová A, Prensier G, Chambouvet I, Florent I, Guillou L (2016) Ultrastructure of *Selenidium pendula*, the type species of archigregarines, and phylogenetic relations to other marine Apicomplexa. Protist 167(4):339–368. https://doi.org/10.1016/j.protis.2016.06.001

Simdyanov TG, Kuvardina ON (2007) Fine structure and putative feeding mechanism of the archigregarine *Selenidium orientale* (Apicomplexa: Gregarinomorpha). Eur J Protistol 43(1):17–25. https://doi.org/10.1016/j.ejop.2006.09.003

Simdyanov TG, Paskerova GG, Valigurová A, Diakin A, Kováčiková M, Schrével J, Gillou L, Dobrovolskij AA, Aleoshin VV (2018) First ultrastructural and molecular phylogenetic evidence from the blastogregarines, an early branching lineage of plesiomorphic Apicomplexa. Protist 169(5):697–726. https://doi.org/10.1016/j.protis.2018.04.006

Soldati D, Foth JB, Cowman AF (2004) Molecular and functional aspects of parasite invasion. Trends Parasitol 20(12):567–574. https://doi.org/10.1016/j.pt.2004.09.009

Stebbings H, Boe GS, Garlick PR (1974) Microtubules and movement in the archigregarine *Selenidium fallax*. Cell Tissue Res 348(3):331–345. https://doi.org/10.1007/BF00224261

Stokkermans TJ, Schwartzman JD, Keenan K, Morrissette NS, Tilney LG, Roos DS (1996) Inhibition of *Toxoplasma gondii* replication by dinitroaniline herbicides. Exp Parasitol 84(3):355–370. https://doi.org/10.1006/expr.1996.0124

Tardieux I, Baum J (2016) Reassessing the mechanics of parasite motility and host-cell invasion. J Cell Biol 214(5):507–515. https://doi.org/10.1083/jcb.201605100

Valigurová A, Vaškovicová N, Diakin A, Paskerova GG, Simdyanov TG, Kováčiková M (2017) Motility in blastogregarines (Apicomplexa): native and drug-induced organisation of *Siedleckia nematoides* cytoskeletal elements. PLoS One 12(6):e0179709. https://doi.org/10.1371/journal.pone.0179709

Valigurová A, Vaškovicová N, Musilová M, Schrével J (2013) The enigma of eugregarine epicytic folds: where gliding motility originates? Front Zool 10(1):57. https://doi.org/10.1186/1742-9994-10-57

Wakeman KC, Horiguchi T (2017) Morphology and molecular phylogeny of the marine gregarine parasite *Selenidium oshoroens*e n. sp. (Gregarina, Apicomplexa) isolated from a northwest pacific hydroides *Ezoensis okuda* 1934 (Serpulidae, Polychaeta). Mar Biodiv 48:1498. https://doi.org/10.1007/s12526-017-0643-1

Wakeman KC, Heintzelman MB, Leander BS (2014) Comparative ultrastructure and molecular phylogeny of *Selenidium melongena* n. sp. and *S. terebellae* Ray 1930 demonstrate niche partitioning in marine gregarine parasites (Apicomplexa). Protist 165(4):493–511. https://doi.org/10.1016/j.protis.2014.05.007

Wetzel DM, Hakansson S, Hu K, Roos D, Sibley LD (2003) Actin filament polymerization regulates gliding motility by apicomplexan parasites. Mol Biol Cell 14:396–406. https://doi.org/10.1091/mbc.e02-08-0458

Whitelaw JA, Latorre-Barragan F, Gras S, Pall GS, Leung JM, Heaslip A, Egarter S, Andenmatten N, Nelson SR, Warshaw DM, Ward GE, Meissner M (2017) Surface attachment, promoted by the actomyosin system of *Toxoplasma gondii* is important for efficient gliding motility and invasion. BMC Biol 15:1. https://doi.org/10.1186/s12915-016-0343-5